

***Enzymatic digestion of luminescent albumin-stabilized gold  
nanoclusters under anaerobic conditions: clues to the quenching  
mechanism.***

Matylda Waćławska<sup>1</sup>, Wojciech Dzwolak<sup>1\*,2</sup>

<sup>1</sup> Faculty of Chemistry, Biological and Chemical Research Centre, University of Warsaw, 1 Pasteur Str., 02-093 Warsaw, Poland.

<sup>2</sup> Institute of High Pressure Physics, Polish Academy of Sciences, Sokołowska 29/37 Str., Warsaw, 01-142 Poland

\* Corresponding author: W. Dzwolak

Phone: +48 22 552 6567

Fax: +48 22 552 4029

E-mail: [wdzwolak@chem.uw.edu.pl](mailto:wdzwolak@chem.uw.edu.pl)

## Abstract

Many of the potential applications of albumin-stabilized gold nanoclusters (AuNC) arise from the sensitivity of their luminescence to the presence of various ions and albumin-degrading proteases. However, the underlying photophysics and the mechanisms responsible for protease-induced quenching of AuNC luminescence are not fully understood. Here, we study proteinase K-induced digestion of bovine serum albumin (BSA)-AuNC conjugate under aerobic and anaerobic conditions. To this end, we adapt a Co(II)-catalyzed sulfite-based protocol enabling effective *in situ* deoxidization without deactivation of the enzyme. In the absence of proteinase K, the anaerobic conditions facilitate luminescence of BSA-AuNC reflected by a moderate increase in the red luminescence intensity. However, in the presence of proteinase K, we have observed a steeper decrease of emission intensity irrespective of whether the digestion was carried out under aerobic or anaerobic conditions. In both cases, the diminishing fluorescence occurred *in phase* with shifting of the emission maximum to longer wavelengths. These results contradict the previous hypothesis that protease-induced quenching of BSA-AuNC luminescence is a consequence of enhanced diffusion of oxygen to bare AuNC. Instead, aggregation of unprotected AuNCs and separation of nanoclusters from albumin's side chains involved in energy transfers and luminescence-promoting electron donors may underlie the observed sensitivity of BSA-AuNC to protease treatment. Our findings are discussed in the context of mechanisms of formation and photophysics of BSA-AuNC conjugates.

## Keywords

Noble metal nanoclusters; luminescence; quenching; oxygen; protease; anaerobic conditions.

## 1. Introduction

The unorthodox, yet effective and facile synthesis of luminescent AuNCs in the form of albumin conjugates developed by Xie *et al*<sup>1</sup> has triggered enormous interest of chemists, physicists and material scientists. Although fundamental studies on tiny clusters of noble metal atoms precede this finding by decades<sup>2-4</sup>, the ease with which albumin-enveloped-AuNCs are created, the sensitivity of their photophysical properties to various factors, and biocompatibility provided by the biomacromolecular carrier inspired numerous efforts aimed at devising new AuNC-based tools for bioimaging, clinical diagnostics and analytical chemistry. Importantly, various biopolymers including other proteins (e.g. lysozyme<sup>5</sup>), peptides<sup>6,7</sup>, and nucleic acids<sup>8</sup> have been demonstrated to have the capacity to act in a manner similar to albumin as co-substrates and stabilizers of AuNCs. The very broad field of potential applications of these systems has been covered in several excellent reviews.<sup>9-15</sup> Surprisingly, while the perspective of real-life applications of albumin-conjugated AuNCs is becoming increasingly clear, the underlying mechanisms through which the complexes are formed and luminescence intensity is affected by changing environmental factors are not understood in sufficient detail.<sup>16-19</sup> In the case of the Xie's protocol involving alkaline pH, BSA acts as both a reducing agent for chloroauric(III) acid and a macromolecular ligand subsequently enveloping formed AuNCs. The latter function is essential, as bare AuNCs are unstable and prone to self-assembly into larger metallic and therefore non-luminescent nanoparticles (AuNPs). Various amino acid side chains on BSA surface are expected to display distinct reactivity towards the Au(III) substrate and the AuNC product.<sup>20-24</sup> Furthermore, the presence of certain chemical groups (some of which may form only as byproducts of the synthesis and are thus absent in the native albumin e.g. dityrosine<sup>25</sup>) capable of engaging in redox processes or resonant energy transfers in the cluster's vicinity may be crucial for maintaining luminescence of BSA-AuNC. The impact of charge transfer from surface ligands on

luminescence is well-recognized beyond the subcategory of albumin-stabilized AuNCs.<sup>26</sup> While luminescence of AuNC is affected by basic physicochemical parameters including temperature, pressure<sup>27</sup> and pH<sup>17</sup>, there are now identified specific cations, e.g. Cu<sup>2+</sup>, Hg<sup>2+</sup><sup>12,28,29</sup>, anions, e.g. nitrite<sup>30</sup>, small molecules e.g. folic acid<sup>31</sup> and proteolytic enzymes<sup>32</sup> which quench luminescence of albumin-enveloped AuNCs very effectively. The magnitude of this effect often strictly depends on the quencher concentration which merits its possible applications as a diagnostic tool. There are multiple mechanisms involved in the quenching phenomenon excellently reviewed elsewhere<sup>14,33</sup>, understood to various degrees. For example, in the case of Cu<sup>2+</sup>-induced quenching of BSA-AuNC luminescence, an intuitive mechanism has been proposed in which copper(II) ions interfere with electron-donating amino acid side chains in albumin's AuNC-binding moiety.<sup>33,34</sup> On the other hand, the case of protease-induced quenching is more intricate.<sup>33</sup> The enzyme action is limited to degradation of the proteinaceous envelope and is not expected to directly affect the redox state of AuNC.<sup>35</sup> Hence, it was proposed that the proteolysis may simply reduce abundance of electron-donating ligands from the surface of AuNCs.<sup>35</sup> An alternative mechanism has been presented, in which molecular oxygen is the actual quencher whereas the protease only facilitates its diffusion to AuNC by degrading the protective albumin envelope.<sup>36</sup> This idea is reminiscent of the oxygen-induced triplet-triplet annihilation upconversion quenching known to affect many light-emitting systems.<sup>37</sup> Our objective was to revisit the phenomenon of protease-induced quenching under conditions preventing secondary interactions of dissolved oxygen with solvent-exposed AuNCs. As the standard methods of removal of oxygen from liquid samples are often ineffective or poorly adaptable to the need to maintain protease activity, here we use a modified approach first described by Hobson et al.<sup>38</sup> in which oxygen is removed *in situ* by a Co(II)-catalyzed reaction with sulfite at a close-to-physiological pH. This approach has allowed us to study the impact of enzymatic digestion of protein envelope

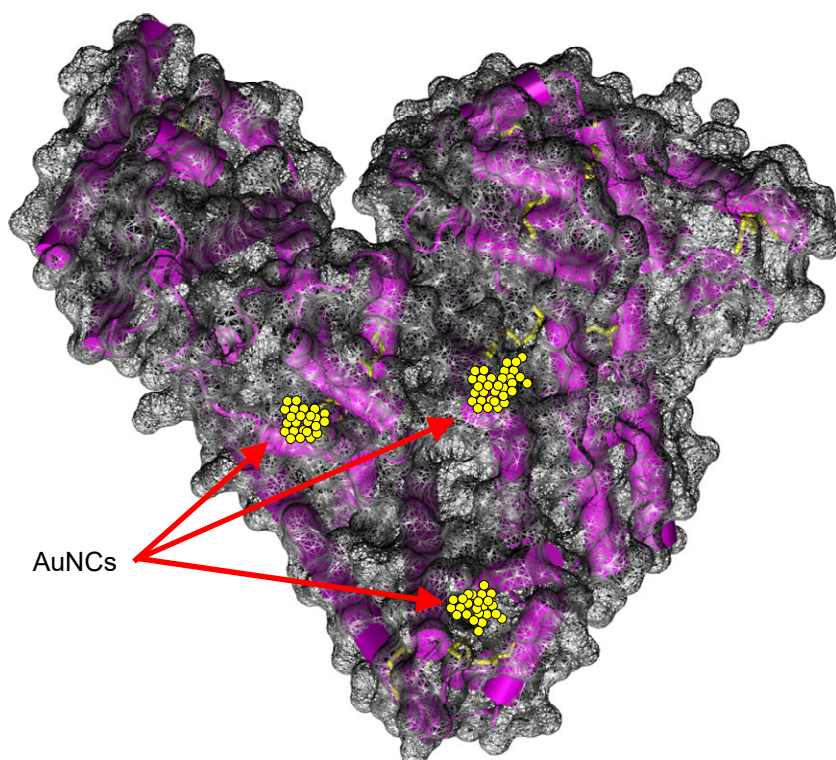
on BSA-AuNC luminescence under strictly anaerobic conditions and therefore draw more unambiguous conclusions regarding the oxygen's role in the quenching.

## 2. Results and Discussion

### *2.1 Susceptibility of BSA-AuNC to enzymatic proteolysis in the presence and absence of sulfite-based deoxidizing solution (DS).*

The harsh conditions of BSA-AuNC synthesis render albumin molecules partly disordered<sup>39</sup>. Still, the surface of the native BSA molecule is often used to map residues which are more likely to become involved in the nesting of AuNCs.<sup>20,21,24</sup> In Fig. 1A, a simplistic visualization of BSA-AuNC conjugate based on the native BSA structure is presented. The protein's amino acid sequence is rich in cysteine, tyrosine, histidine, and methionine residues which are important for the formation of luminescent conjugate (Fig. 1B). In this study, we have selected proteinase K as a robust non-specific protease capable of digesting BSA at multiple sites. The choice was also affected by the necessity to match a BSA-AuNC-degrading enzyme to deoxidization conditions that would not diminish its activity. The outcome of preliminary experiments on digestion of BSA-AuNC with proteinase K under aerobic conditions is reported in Fig. 2. An addition of proteinase K to BSA-AuNC at the 100:1 albumin: enzyme mass ratio results in a noticeable decrease in the luminescence intensity after 1 hour of incubation at 37 °C. The luminescence is hardly visible after 24 hours long incubation under the same conditions. When a non-digested BSA-AuNC sample is placed in a dialysis bag (with the membrane's molecular weight cut-off of 14 kDa) submerged in water there is no evidence of the conjugate permeating to the outside solution after 24 hours of dialysis (Fig. 2B). In Fig. 2C, UV-VIS absorption spectra collected for the inside and outside solutions after 24 hours of dialysis of digested and non-digested BSA-AuNC are presented.

A



B

DTHKSEI A HRF KDL GEEHF KGLV L I A F SQY LQQCPF DEHV KL V NEL TEF A KTCV A DESHA GCEKSL HTL F  
 GDEL CKV A SL RETY GDMA DCEKQEPERNECF L SHKDDSPDL PKL KPDPNTL CDEF KA DEKKF W GK Y L Y EI  
 A RRHPY F Y A PEL L Y Y A NK Y NGV F QECCQA EDKGA CL L PKI ET M REKV L A SSA RQRL RCA SI QKF GERA  
 L KA W SV A RL SQKF PKA EF V EV TKL V TDL TKV HKECCHGDL L ECA DDRA DL A KY I CDNQDTI  
 SSKLKECCDKPL L EKSHCI A EV EKDA I PENL PPL TA DF A EDKDV CKNY QEA KDA F L GSF L Y EY SRRHPEY A  
 V SV L L RL A KEY EA TL EECCA KDDPHA CY STV F DKL KHL V DEPQNL I KQNCQDF EKL GEY GF QNA L I V  
 RY TRKV PQV STPTL V EV SRSL GKV GTRCCTKPESER MPCTEDY L SL I L NRL CV L HEKTPV SEKV TKCTESL V  
 NRRPCF SA L TPDETY V PKA F DEKL F TF HA DI CTL PDTEKQI KKQTA L V EL L KHKKA TEEQL KTV M ENF V A  
 F V DKCCA A DDKEA CF A V EGPKL V V STQTA LA

**Figure 1.** (A) Simplistic structural visualization of BSA-AuNC conjugate (PDB entry 4F5S), according to <sup>24</sup>. (B) Amino acid sequence of BSA. Amino acid residues essential for AuNC binding are marked in red (Cys), green (His), magenta (Met), and blue (Tyr) – according to <sup>20,21</sup>; yellow vertical lines mark cleavage sites for proteinase K.

The elevated baseline above 300 nm that extends well into the visible wavelength range arises from overlapping various electronic transitions within AuNCs and their immediate molecular surroundings. We note that the magnitude of this broad absorption does not change significantly due to the digestion when the spectra corresponding to the inside solutions after

24 hours of incubation are compared. This is accordance with the naked-eye observation that the whole yellow-colored content remains within the bag throughout the dialysis.

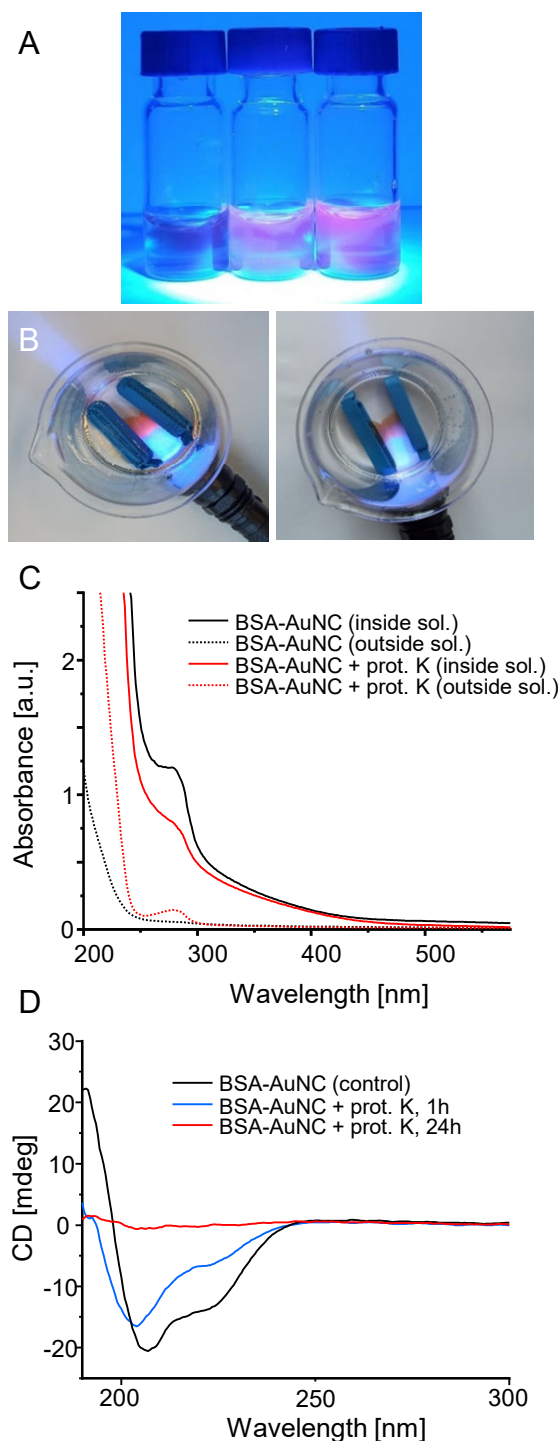


**Figure 2.** (A) 1 wt. % BSA-AuNC solution with and addition of  $10^{-2}$  wt. % proteinase K illuminated with 365 nm UV light; the vessels from left to right contain samples digested for 24 h, 1 h, and 0 min at pH 7.5 and 37 °C. (B) Dialysis bags containing the same BSA-AuNC + proteinase K mixed solution submerged in deionized water before (left) and after 24 h long digestion; dialysis membrane's molecular weight cut-off (MWCO) was 14 kDa. (C) UV



absorption spectra of dialysate (sample placed inside dialysis bag – solid lines) and outside dialysate solution (dotted lines) after 24 h of dialysis; BSA-AuNC was subjected to prior 24 h long digestion with proteinase K at pH 7.5 and 37 °C (red line), the volume of the outside deionized water was 10 times of the dialysate; spectra corresponding to control undigested BSA-AuNC sample are black; the inside solutions were diluted 10 times prior to spectral measurements. (D) Far UV-CD spectra of BSA-AuNC digested with proteinase K for 1 and 24 h (pH 7.5 and 37 °C; 1:100 enzyme: BSA mass ratio) compared with the spectrum of control non-digested BSA-AuNC sample.

Remarkably, UV absorption at approximately 280 nm arising from BSA's aromatic residues (mostly tyrosine side chains) of the inside solution of pre-digested sample decreases after the round of dialysis. Clearly, the proteolysis results in a release of small peptide fragments containing tyrosine residues which permeate to the outside solution. Accordingly, absorbance at 280 nm is clearly detected in the corresponding outside solution which also features a very steep increase in UV absorption below 240 nm – corresponding to the much stronger absorption by backbone amide chromophores. Hence the proteolysis by proteinase K separates small peptide fragments rich in the amino acid involved in possible energy/electron transfers to AuNC but the nanoclusters themselves remain bound to larger albumin parts. Subsequently, we used far-UV circular dichroism to probe conformational changes in BSA caused by the treatment with proteinase K. The double minimum at 208/222 nm visible in the CD spectrum of BSA-AuNC collected before digestion (Fig. 2D) is indicative of the dominant  $\alpha$ -helical conformation even though its content in the conjugate is reduced relative to the native protein.<sup>39</sup> The fact that, unlike in native BSA, the CD intensity at 208 nm is roughly by one third higher than at 222 nm reflects the partial unfolding and destabilization of the helical fold taking place upon synthesis of the conjugate. The two superimposed spectra correspond to BSA-AuNC digested to 1 and 24 hours with proteinase K. Even the shorter digestion is sufficient to significantly disrupt the residual helical structure which is reflected both by exacerbated decay of the 222 nm component and the overall decrease of CD signal. The flat

CD spectrum collected after 24 hours of proteolysis is consistent with the inability of short peptide fragments to adopt any defined secondary structures.

The application of proteinase K as an effective BSA-AuNC-degrading proteolytic enzyme for this study's goal is conditioned on its activity in the presence of chemicals required for the *in situ* deoxidization. The alkaline pH of concentrated aqueous sodium sulfite typically used for this purpose would strongly affect the enzymes activity. On the other hand, the protocol proposed by Hobson and colleagues<sup>38</sup> allows one to conduct a very effective deoxidization using relatively diluted sodium sulfite at the close-to-physiological pH of 7.5 with  $\text{Co}^{2+}$  cations acting as the catalyst. As the Hobson's method was initially developed for and tested on aqueous solutions of inorganic salts there was a possibility that the addition of proteins would significantly reduce its effectiveness through complexation of  $\text{Co}^{2+}$  with certain amino acid side chains (e.g. of histidine). We have addressed this problem by modifying the Hobson's protocol and increasing the concentration of  $\text{Co}^{2+}$  added. Figure 3 shows how progress of the chemical deoxidization by the sulfite/ $\text{Co}^{2+}$  system is affected by addition BSA-AuNC and native BSA. While the presence of either proteinaceous solute slows down the process (under the conditions compatible with follow-up spectroscopic measurements) it is still completed within at most 10 minutes (5 min in the case of BSA-AuNC). Next, SDS-PAGE electrophoresis was used to assess activity of proteinase K in the presence of DS. It was reported earlier that the synthesis of BSA-AuNC is accompanied by agglomeration of the protein into larger oligomers which remain nevertheless more susceptible to enzymatic proteolysis than native BSA<sup>39</sup>. As shown in the inset of Fig. 3, most of these large oligomers of molecular weight exceeding 250 kDa do not even enter the polyacrylamide gel phase. In the presence of proteinase K, these assemblies are degraded to a heterogeneous mixture of protein fragments manifesting as long faint smears. Importantly, the degradation appears not to be inhibited when carried out in the presence of DS. Thus the

results presented in Fig. 3 clearly indicate that proteinase K-based degradation of BSA-AuNC can be carried out in the sulfite/ $\text{Co}^{2+}$  DS without significant deceleration of the oxygen removal and without inactivation of the protease.

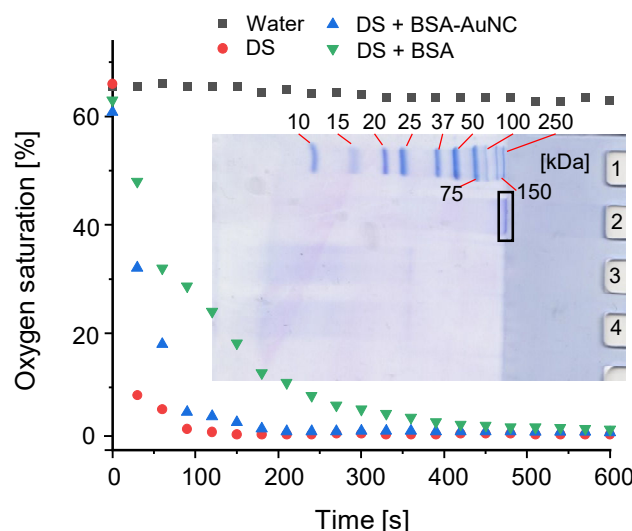


**Figure 3.** Kinetics of oxygen depletion in aqueous 1 wt. % BSA-AuNC samples in the presence of sulfite- $\text{Co(II)}$  deoxidizing solution (DS: 15 mM sodium sulfite, 32  $\mu\text{M}$   $\text{CoCl}_2$ , pH 7.5, 37  $^\circ\text{C}$ ). Control experiments were conducted using deionized water, solution of native BSA in water, and neat DS. Inset: SDS-PAGE test of proteinase K activity toward BSA-AuNC in the DS. The following lanes correspond to marker (1), non-digested BSA-AuNC (2), the aggregated complex does not enter the gel – indicated with black frame, BSA-AuNC digested with proteinase K in the absence (3) and presence (4) of the DS. The digestion of 1 wt. % BSA-AuNC with proteinase K was carried out for 24 h at pH 7.5, 37  $^\circ\text{C}$  at 1:100 conjugate: protease mass ratio in sealed vessels.

## 2.2 BSA-AuNC luminescence subjected to enzymatic proteolysis under aerobic and anaerobic conditions.

Having established the conditions under which both enzymatic digestion of BSA-AuNC and deoxidization could take place simultaneously in a sealed anaerobic optical cuvette, we have carried out the key experiment of this study. In Fig. 4, time-lapse emission spectra of BSA-AuNC's luminescence excited at 365 nm are shown. In control experiments,

alternatively only deoxidization (panel A), or digestion under aerobic conditions (panel B) took place.

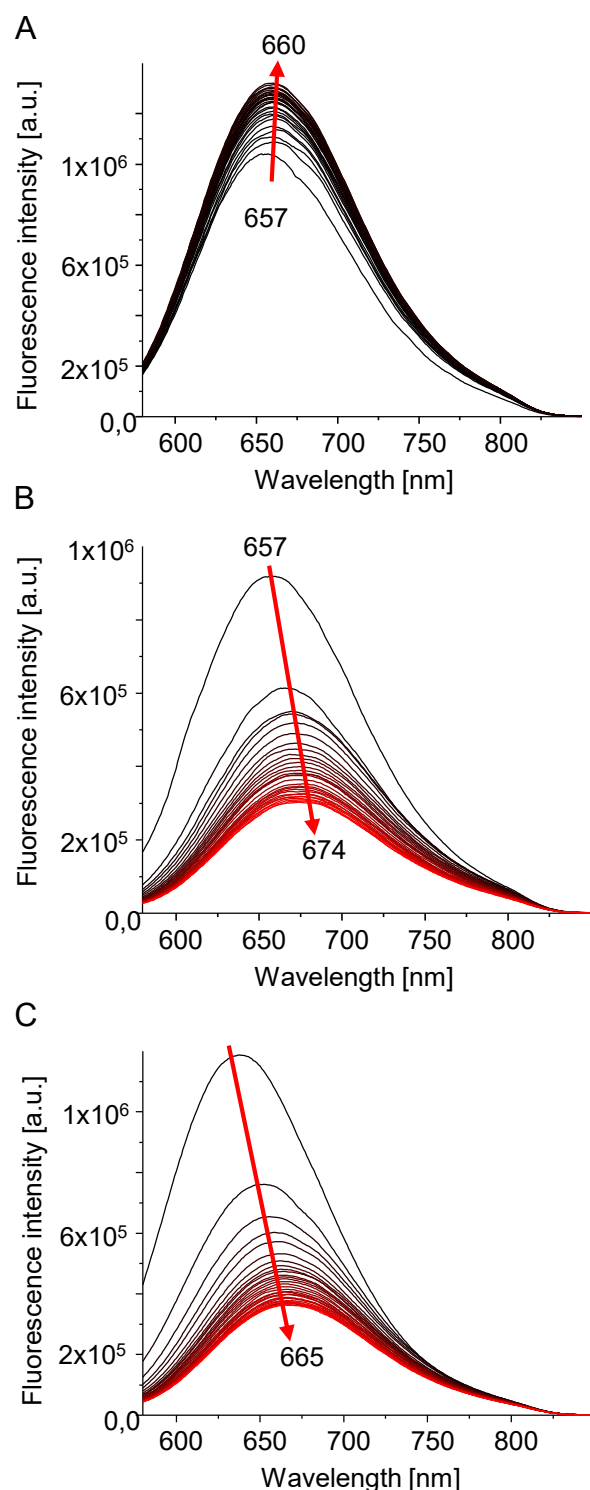


**Figure 4.** Time-lapse emission spectra of BSA-AuNC (1 wt. %, pH 7.5, 37 °C) excited at 365 nm and collected at 10 min. intervals for the period of 5 hours. (A) in DS (15 mM  $\text{Na}_2\text{SO}_3$ , 32  $\mu\text{M}$   $\text{CoCl}_2$ ); (B) in water in the presence of  $2 \times 10^{-2}$  wt. % proteinase K; (C) in DS and in the presence of  $2 \times 10^{-2}$  wt. % proteinase K. An anaerobic quartz cuvette with a 10 mm optical

pathway was used. The dead time between mixing of all components and collecting the first spectrum in each series was 13 minutes.

In the first case, a moderate time dependent increase (by roughly  $\sim 20\%$  over the period of 5 hours) in luminescence intensity is accompanied by an insignificant red-shift of the emission maximum. When BSA-AuNC is degraded by proteinase K in the presence of dissolved oxygen, luminescence monotonically decreases and the emission maximum undergoes a more pronounced shift to longer wavelengths (above 674 nm after 5 hours). Importantly, when the BSA-AuNC conjugate is mixed with both DS and proteinase K at the beginning of the measurements, the course of spectral changes is very similar to those observed when the digestion takes place under aerobic conditions (Fig. 4 C), i.e.: the luminescence intensity steadily decreases while the maximum is shifting to longer wavelengths. Interestingly, the moderate increase of luminescence shown in Fig. 4 A occurs at longer time scales than the deoxidization under very similar sample conditions selected for the control experiment employing an electrochemical oxygen sensor (Fig. 3). This may be due to interplay of several factors. For example, the sensitivity of AuNC to quenching by oxygen may be higher than that of the sensor and thus the deoxidization reaction may require more time when monitored by BSA-AuNC luminescence. In addition, the sulfite ions present in the DS may also restrain conformational dynamics of fluctuating, partly disordered BSA envelope (acting as a Hofmeister series anion<sup>40</sup>) which could affect the efficiency of protein-AuNC energy transfers. Such a process could, in principle, for a heterogeneous and partly agglomerated system which is BSA-AuNC, occur at longer timescales and contribute to the observed slow luminescence increase. The decrease in luminescence intensity caused by the proteolytic degradation of BSA-AuNC is accompanied by the shifting of emission maximum to longer wavelengths regardless of the presence of DS (Fig. 4). We have collected excitation-emission maps for the intact and partially digested BSA-AuNC in the presence of oxygen (Fig. 5).

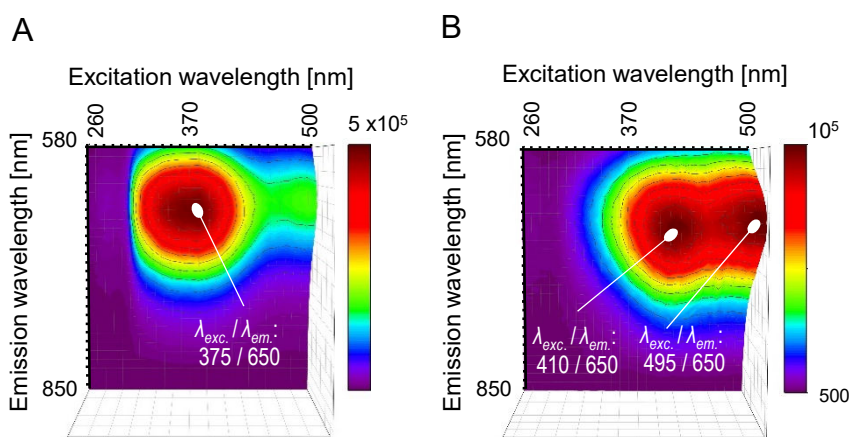


**Figure 5.** Excitation-emission maps of BSA-AuNC collected in the presence of water-dissolved oxygen: intact (A) and after 4 hours of digestion with proteinase K (B). The sample and measurement conditions were the same as in Fig. 4

Interestingly, the map obtained for the digested sample reveals splitting of the main maximum, suggesting the presence of two distinct populations of AuNC. Hypothetically, one of these populations could be AuNCs bound to peptide fragments relatively depleted (due to the proteolysis) of aromatic amino acid residues involved in energy transfers. Luminescence of these AuNC is not only less effective, but may also rely to a higher degree on a direct excitation at longer wavelengths. Further proteolysis could release unstable ‘bare’ AuNCs with a pronounced tendency to agglomerate into non-luminescent AuNPs.

Additional clues about the absence of the interplay of oxygen and proteolytic degradation in quenching of BSA-AuNC luminescence were obtained from another kinetic experiment in which proteinase K and DS were added separately and in varying order (Fig. 6). Hence the anaerobic conditions and proteolysis were ‘switched on’ at a certain point of experiment (after 140 minutes) consisting of continuous measurements of thermostated BSA-AuNC samples sealed in anaerobic cuvettes. Incubation of the conjugate under anaerobic conditions in DS is accompanied by slow and rather insignificant changes in emission band’s position, intensity and spectral centroid. The late addition of concentrated proteinase K causes

rapid changes of all these spectral parameters associated with quenching of the luminescence (Fig. 6A).

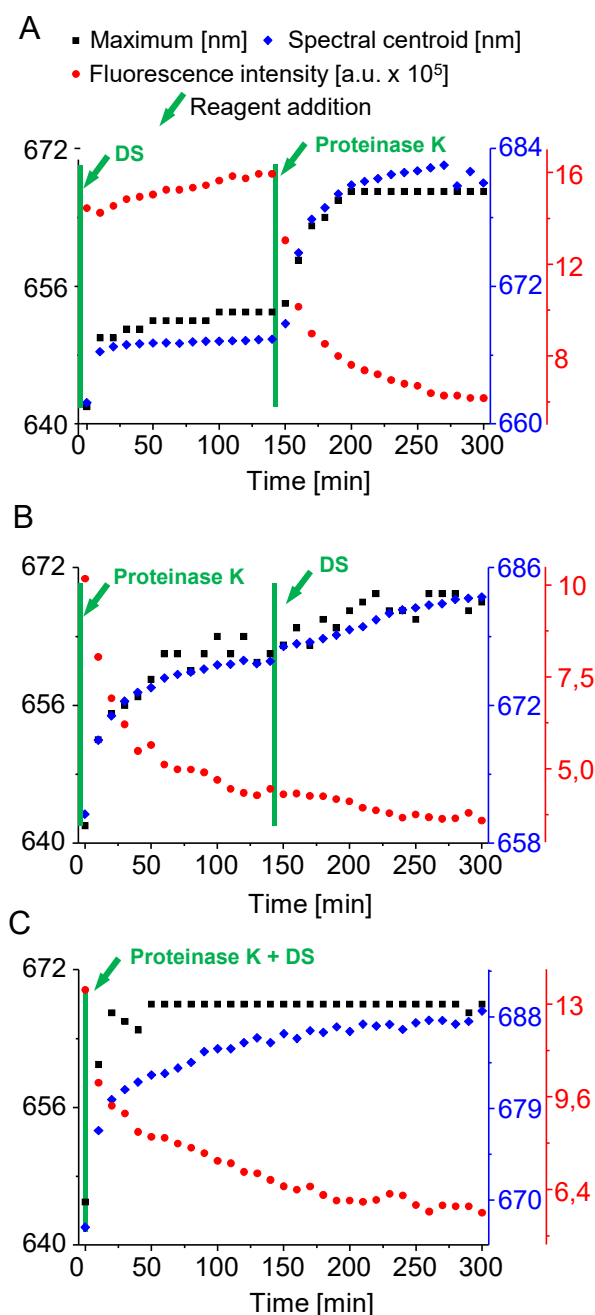


**Figure 6.** Impact of different scenarios of delayed addition of proteinase K and DS on luminescence of BSA-AuNC reflected by time-dependent changes in the emission band's position, center of mass, and intensity. (A) Temporal evolution of luminescence of 0.5 wt. % BSA-AuNC in DS. After 140 minutes proteinase K is added to the final BSA-AuNC: enzyme mass ratio of 50:1 (green arrow). (B) A reversed mixing order: luminescence changes of 0.5 wt. % BSA-AuNC in water in the presence of proteinase K (50:1 mass ratio); after 140 minutes concentrated DS is added (green arrow) to give the ultimate sample composition the same as in (A). (C) Control experiment in which all ingredients: BSA-AuNC, DS, and

proteinase K are present from the start at the concentrations the same as in (A) and (B). Other conditions: excitation at 365 nm; pH 7.5, 37 °C, continuous stirring, samples are incubated in a sealed anaerobic 10 mm quartz cuvette.

When the order of mixing is reversed the obtained results are consistent with the scenario in which not the oxygen but the proteolysis itself causes quenching. The late addition of DS to an already partially digested BSA-AuNC does not reverse the trends of spectral changes (Fig. 6B) which are, in fact, quite similar to those observed when both the enzyme and DS are present in the samples from the very beginning (Fig. 6C).

### 3. Conclusions

In summary, our approach enabled investigation of enzymatic proteolysis of BSA-AuNC under strictly anaerobic conditions permissive to high enzyme's activity. While the chemical removal of water-dissolved oxygen does moderately increase the luminescence of intact BSA-AuNC, it does not prevent the profound quenching caused by the degradation. Our results show clearly that the proteinase K-induced luminescence decay does not rely on dissolved oxygen as the actual quencher. The results are consistent with the alternative explanations of the protease actions in which protease-mediated removal of certain amino acids (e.g. tyrosine) from AuNC's vicinity and possibly subsequent agglomeration of AuNCs into non-luminescent AuNPs underlie the quenching process. It is clear that the emerging applications of albumin-protected AuNCs<sup>28-32, 42</sup> will only benefit from a better understanding of the mechanisms underlying the environment-sensitive luminescence of these entities. This knowledge is urgently needed to increase selectivity and specificity of AuNC-based sensors.

### 4. Materials and Methods

#### *4.1. Materials and preparation of BSA-AuNC samples*



BSA,  $\text{HAuCl}_4 \cdot 3\text{H}_2\text{O}$ , proteinase K and other chemicals of the analytical grade were purchased from Sigma-Aldrich (St. Louis, MO, USA) and used without further purification. BSA-AuNC conjugate was synthesized according to the protocol originally developed by Xie et al.<sup>1</sup>: 500  $\mu\text{l}$  volumes of aqueous solutions of  $\text{HAuCl}_4$  (10 mM) and BSA (50 mg/mL) were mixed vigorously at 37 °C for 2 minutes after which a 50  $\mu\text{l}$  portion of 1 M aqueous NaOH was added. The thus obtained solution was again mixed and subjected to 12 hours long agitation (600 rpm) at 37 °C in an Eppendorf Thermomixer Comfort accessory which resulted in the formation of BSA-AuNC. Digestion with proteinase K (cat. no. P203-25MG, batch no. 0000089941, nominal activity  $\geq 30$  units/mg) was carried out using freshly prepared enzyme solutions at pH 7.5 and 37 °C, other details are specified in figure captions. As routine methods of deoxidization may be poorly adaptable to viscous protein-rich solutions in which protease activity must be maintained we have selected a modified approach first described by Hobson et al.<sup>38</sup> The method employs *in situ* chemical deoxidization through a Co(II)-catalyzed oxidation of sulfite at a close-to-physiological pH. Because dissolved proteins tend to bind and remove  $\text{Co}^{2+}$  ions from the solution in the protocol applied in this study, the concentration of Co(II) is increased compared to the conditions used by Hobson et al. Typically, deoxidization was achieved by dissolving BSA-AuNC and proteinase K in 15 mM sodium sulfite, 22  $\mu\text{M}$   $\text{CoCl}_2$ , pH 7.5.

## 4.2. Methods

### 4.2.1. Spectroscopic measurements.

Luminescence of BSA-AuNC was measured on a FLS980 fluorescence spectrometer from Edinburgh Instruments, UK equipped with a Peltier temperature control accessory and a magnetic stirrer. Typically, emission spectra were excited at 365 nm (Figures 4 and 6). The wavelength range used for the excitation-emission maps is indicated in Figure 5. All

measurements were carried out at 37 °C for samples placed in a sealed anaerobic 10 mm quartz cuvette (from Hellma Analytics, Müllheim, Germany) and gently agitated *in situ* using a magnetic stirrer. UV-VIS absorption spectra shown in Figure 2C were collected at room temperature on an Evolution 220 spectrometer from Thermo Fisher Scientific (Waltham, MA, USA) using 2 nm monochromator bandwidth setting and the scanning rate of 1200 nm/min and 10 mm quartz cuvette. Far-UV circular dichroism (CD) measurements were carried out at 25 °C on samples containing BSA-AuNC at the 0.025 wt. % concentration placed in a 1 mm quartz cuvette (the stock solutions were diluted 40 times with deionized water prior to spectra acquisition). The spectra were collected on Jasco J-815 S spectropolarimeter (Jasco Corporation, Tokyo, Japan) at the 200 nm/min scanning rate. Other details were described earlier.<sup>39</sup>

#### *4.2.2. Sodium dodecyl sulphate–polyacrylamide gel electrophoresis (SDS PAGE)*

The freshly prepared 1 mg/ml solution of proteinase K (from Sigma-Aldrich) in water was pH-adjusted to 7.5. After establishing optimal conditions for the digestion assay, the enzyme was added to BSA-AuNC liquid samples either in deionized water or in DS, pH-pre-adjusted in either case to 7.5. Digestion was carried out at 100 : 1 BSA-AuNC : proteinase K mass ratio at 37°C for 24 hours. SDS-PAGE-based analysis of digested protein samples was carried out according to the protocol by Laemmli.<sup>41</sup> Immediately after proteolysis, 50 µl of a sample was added to 50 µl of SDS-PAGE sample buffer (125 mM TrisHCl, pH 6.8, 20% glycerol, 4% SDS, 0.1% bromophenol blue and incubated at 100 °C for 3 min. Subsequently, 7.5 µL portion of protein sample (corresponding to 7.5 µg of BSA per lane) was loaded on 12% polyacrylamide gel. The electrophoresis was carried out using Hoefer SE250 Mini-vertical gel electrophoresis unit and PS600 Power Supply. The gel was run in running buffer

(25 mM TrisHCl, 192 mM glycine, 0.1% SDS, pH 8.3) at a constant current of 30 mA. Protein bands were visualized by Coomassie staining.

#### *4.2.3. Dissolved oxygen measurements.*

Dissolved oxygen was monitored using a CO-411 amperometric device coupled to a COG-1 electrochemical oxygen sensor both from ELMETRON, Poland.

### Acknowledgments:

This work was supported by the National Science Centre of Poland, grant no. 2017/25/B/ST5/02599. The work was conducted in part at the Biological and Chemical Research Centre, University of Warsaw, established within the project co-financed by EU from the European Regional Development Fund under the Operational Programme Innovative Economy.

### Conflict of Interest

The authors declare no conflict of interests.

### Author Contributions

**Wojciech Dzwolak:** conception, design, funding acquisition, analysis of data, writing - original draft, project administration; **Matylda Wacławska:** research and data collection, analysis of data

### References

1 J. Xie, Y. Zheng and J. Ying, *J. Am. Chem. Soc.*, 2009, **131**, 888–889.

- 2 Malatesta L, Naldini L, Simonetta G, Cariati F. *Chem. Commun.* 1965;0:212–3.
- 3 R. Jin, *Nanoscale*, 2010, **2**, 343–362.
- 4 F. Gröhn, B. Bauer, Y. Akpalu, C. Jackson and E. Amis, *Macromolecules*, 2000, **33**, 6042–6050.
- 5 D. Lu, L. Liu, F. Li, S. Shuang, Y. Li, M. M. F. Choi and C. Dong, *Spectrochim. Acta A*, 2014, **121**, 77–80.
- 6 Y. Gu, Q. Wen, Y. Kuang, L. Tang and J. Jiang, *RSC Adv.*, 2014, **4**, 13753–13756.
- 7 Q. Yuan, Y. Wang, L. Zhao, R. Liu, F. Gao, L. Gao and X. Gao, *Nanoscale*, 2016, **8**, 12095–12104.
- 8 G. Liu, Y. Shao, K. Ma, Q. Cui, F. Wu and S. Xu, *Gold Bull.*, 2012, **45**, 69–74.
- 9 C. A. Lin, T. Y. Yang, C. H. Lee, S. H. Huang, R. A. Sperling and M. Zanella, *ACS Nano*, 2009, **3**, 395–401.
- 10 L. Shang, S. Dong and G. Nienhaus, *Nano Today*, 2011, **6**, 401–418.
- 11 D. M. Chevrier, A. Chatt and P. Zhang, *J. Nanophotonics*, 2012, **6**, 064504.
- 12 Y. Zheng, L. Lai, W. Liu, H. Jiang and X. Wang, *Adv. Colloid Interface Sci.*, 2017, **242**, 1–16.
- 13 Y. Zheng, J. Wu, H. Jiang and X. Wang, *Coordin. Chem. Rev.*, 2021, **431**, 213689.
- 14 Y. Xiao, Z. Wu, Q. Yao and J. Xie, *Aggregate*, 2021, **2**, 114–132.
- 15 Y. Bai, T. Shu, L. Su and X. Zhang, *Crystals*, 2020, **10**, 357.
- 16 E. Oh, A. L. Huston, A. Shabaev, A. Efros, M. Currie and K. Susumu, *Sci. Rep.*, 2016, **6**, 35538.
- 17 J. M. Dixon and S. Egusa, *J. Am. Chem. Soc.*, 2018, **140**, 2265–2271.
- 18 B. A. Russell, B. Jachimska, I. Kralka, P. A. Mulheran and Y. Chen, *J. Mater. Chem. B*, 2016, **4**, 6876–6882.
- 19 J. M. Dixon and S. Egusa, *J. Phys. Chem. C*, 2019, **123**, 10094–10100.

- 20 Y. N. Tan, J. Y. Lee and D. I. Wang, *J. Am. Chem. Soc.*, 2010, **132**, 5677–5686.
- 21 A. A. Buglak and A. I. Kononov, *RSC Adv.*, 2020, **10**, 34149–34160.
- 22 X. Li, N. Li and L. Zhao, *Sci. Bull.*, 2016, **61**, 1732–1738.
- 23 H. Cai and P. Yao, *Colloid. Surface. B*, 2014, **123**, 900–906.
- 24 B. A. Russell, K. Kubiak-Ossowska, P. A. Mulheran, D. J. S. Birch and Y. Chen, *Phys. Chem. Chem. Phys.*, 2015, **17**, 21935–21941.
- 25 L. Su, T. Shu, J. Wang, Z. Zhang and X. Zhang, *J. Phys. Chem. C*, 2015, **119**, 12065–12070.
- 26 Z. Wu and R. Jin, *Nano Lett.*, 2010, **10**, 2568–2573.
- 27 Q. Li, D. Zhou, J. Chai, W. Y. So, T. Cai, M. Li and R. Jin, *Nat. Commun.*, 2020, **11**, 1–9.
- 28 B. Aswathy and G. Sony, *Microchem. J.*, 2014, **116**, 151–156.
- 29 X. Yu, W. Liu, X. Deng, S. Yan and Z. Su, *Chem. Eng. J.*, 2018, **335**, 176–184.
- 30 B. Unnikrishnan, S. C. Wei, W. J. Chiu, J. Cang, P. H. Hsu and C. C. Huang, *Analyst*, 2014, **139**, 2221–2228.
- 31 B. Hemmateenejad, F. Shakerizadeh-shirazi and F. Samari, *Sensor. Actuat. B-Chem.*, 2014, **199**, 42–46.
- 32 L. Hu, S. Han, S. Parveen, Y. Yuan, L. Zhang and G. Xu, *Biosens. Bioelectron.*, 2012, **32**, 297–299.
- 33 H. Li, W. Zhu, A. Wan and L. Liu, *Analyst*, 2017, **142**, 567–581.
- 34 K. Selvaprakash and Y. C. Chen, *Biosens. Bioelectron.*, 2014, **61**, 88–94.
- 35 J. Zhang, Z. Zhang, X. Nie, Z. Zhang, X. Wu, C. Chen and X. Fang, *J. Nanosci. Nanotechnol.*, 2014, **14**, 4029–4035.
- 36 Y. Wang, Y. Wang, F. Zhou, P. Kim and Y. Xia, *Small*, 2012, **8**, 3769–3773.
- 37 L. Huang, T. Le, K. Huang and G. Han, *Nat. Commun.*, 2021, **12**, 1–9.

- 38 D. B. Hobson, P. J. Richardson, P. J. Robinson, E. A. Hewitt and I. Smith, *Ind. Eng. Chem. Res.*, 1987, **26**, 1818–1822.
- 39 M. Kluz, H. Nieznańska, R. Dec, I. Dziecielewski, B. Niżyński, G. Ścibisz and W. Dzwolak, *PloS one*, 2019, **14**, 0218975.
- 40 C. P. Schwartz, J. S. Uejio, A. M. Duffin, A. H. England, D. N. Kelly, D. Prendergast and R. J. Saykally, *P. Natl. Acad. Sci. U.S.A.*, 2010, **107**, 14008–14013.
- 41 U. K. Laemmli, *Nature*, 1970, **227**, 680–685.
- 42 A. Nain, Y. T. Tseng, Y. S. Lin, S. C. Wei, R. P. Mandal, B. Unnikrishnan, H. T. Chang, *Sensor. Actuat. B-Chem.*, 2020, **321**, 128539.